JPE 16-2-21

http://dx.doi.org/10.6113/JPE.2016.16.2.610
ISSN(Print): 1598-2092 / ISSN(Online): 2093-4718

An Optimized PI Controller Design for Three Phase PFC Converters Based on Multi-Objective Chaotic Particle Swarm Optimization

Xin Guo*, Hai-Peng Ren†, and Ding Liu*

*,†Shaanxi Key Laboratory of Complex System Control and Intelligent Information Processing, Xi'an University of Technology, Xi'an, China

Abstract

The compound active clamp zero voltage soft switching (CACZVS) three-phase power factor correction (PFC) converter has many advantages, such as high efficiency, high power factor, bi-directional energy flow, and soft switching of all the switches. Triple closed-loop PI controllers are used for the three-phase power factor correction converter. The control objectives of the converter include a fast transient response, high accuracy, and unity power factor. There are six parameters of the controllers that need to be tuned in order to obtain multi-objective optimization. However, six of the parameters are mutually dependent for the objectives. This is beyond the scope of the traditional experience based PI parameters tuning method. In this paper, an improved chaotic particle swarm optimization (CPSO) method has been proposed to optimize the controller parameters. In the proposed method, multi-dimensional chaotic sequences generated by spatiotemporal chaos map are used as initial particles to get a better initial distribution and to avoid local minimums. Pareto optimal solutions are also used to avoid the weight selection difficulty of the multi-objectives. Simulation and experiment results show the effectiveness and superiority of the proposed method.

Key words: Chaotic particle swarm optimization, Pareto optimal solution, PI parameters, Spatiotemporal chaos map lattice, Three phase PFC converter

I. INTRODUCTION

As a type of improved three phase Pulse-Width Modulation (PWM) converter, the compound active clamp zero voltage soft switching (CACZVS) three-phase power factor correction (PFC) converter [1] has wide application prospects, because it can realize zero voltage soft switching for all of the switches (including auxiliary switch) and suppress the diode reverse recovery current to reduce power losses.

Traditionally, a three phase PWM converter employs a Proportional Integral (PI) controller based on the synchronous rotating coordinate frame [2]. Using this control configuration, there are three PI controllers including the outer loop output DC voltage controller, the inner loop active current controller and the reactive current controller. Therefore, there are six control parameters that need to be determined to get good performance including a unity power factor, fast transient response and zero steady state error. These parameters are mutual influenced to obtain good performance. References [3] and [4] introduced some PI parameter calculation methods. Reference [5] also proposed an improved parameters tuning algorithm. However, the PI parameters obtained by these methods can only be used as a starting point for parameter tuning. It is necessary to further tune the PI parameters depending on designer experience to get satisfactory performance. In addition to the conventional PI control, many control methods have been proposed recently to improve the performance of three-phase PWM converters [6]-[10]. However, the difficulty of controller parameters tuning limits, to a certain extent, the performance of these control algorithms in practical applications. To avoid the above difficulty, fuzzy logic [11], genetic algorithm (GA) [12], and particle swarm optimization (PSO) theory [13], [14] have been applied to controller design and parameters optimization. However, the control parameter optimization of three phase PWM converters

Manuscript received Jul. 6, 2015; accepted Nov. 16, 2015
Recommended for publication by Associate Editor Se-Kyo Chung.
†Corresponding Author: renhaipeng@xaut.edu.cn
Tel: +86-29-82312401, Xi'an University of Technology
*Shaanxi Key Laboratory of Complex System Control and Intelligent Information Processing, Xi'an University of Technology, China

are a multi-dimensional (six-parameters) and multi-objective (including the unity power factor, fast transient response and zero steady state error) optimization problem, which is still a challenging task.

Generally speaking, there are two main problems restricting advanced optimization algorithms from getting good results. Firstly, to deal with a multi-objective condition, the traditional method gives different weights to different objectives. However, weights selection is very difficult. Secondly, the initial individual distribution has an important impact on the performance of optimization algorithms. In the case of the PSO method, a non-uniform distribution of the initial particles decreases the global convergence performance. To deal with the first problem, reference [14] proposed using the PSO method and the Pareto optimal solution theory to overcome the difficulty of weights selection. For the second problem, because the uniform distribution of the initial particles in the solution space accelerates the convergence speed and reduces the possibility of falling into a local optimum [15], references [16], [17] use chaotic maps to produce the initial particles, where the ergodic characteristic of the chaotic maps was used to get uniform distribution. However, the traditional chaotic map, such as the logistic map [18] and the self-logical map [19], can only achieve a one-dimensional uniform distribution of the particles. With an increasing number of parameters, the uniform distribution of the initial particles in the multi-dimensional solution space is required.

In this paper, an improved CPSO method is proposed for the optimization of the triple closed-loop PI controller parameters for CACZVS three-phase PFC converters. In the proposed method, a spatiotemporal chaos model, referred to as unilateral coupled map lattices, is used to produce multi-dimensional initial particles. The Pareto optimal solution theory is used to avoid the difficulty of weight selection and to achieve balance among the different control objectives such as a unity power factor, fast transient response and zero steady state error. When compared to the conventional random initialization method and the traditional logistic map initialization method, the proposed particles initialization method improves the global searching ability and reduces the time consumption. When compared to the weighted multi-objective optimization method, the proposed method avoids the difficulty of weight selection, and gets automatic balance among the different objectives. Simulation and experiment results verify the effectiveness and superiority of the proposed method.

This paper is organized as follows: Section II gives a brief analysis of the working principle of a CACZVS three-phase PFC converter and its mathematical model; Section III gives the PI controller design for the current loop and voltage loop in detail; Section IV gives the proposed multi-parameter multi-objectives CPSO algorithm; Section V gives a comparison of the simulation and prototype experimental results to show the effectiveness and superiority of the proposed method; Section VI gives some conclusions.

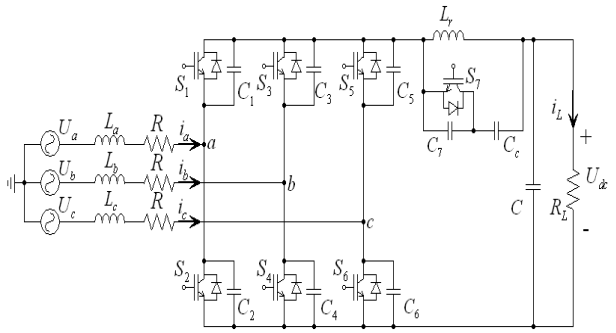

Fig. 1. CACZVS three-phase PFC rectifier.

II. THREE PHASE PFC CONVERTER AND ITS MATHEMATICAL MODEL

The CACZVS three-phase PFC rectifier circuit topology is shown in Fig. 1, where U_a, U_b, and U_c denote the three-phase input voltages; i_a, i_b, and i_c denote the three-phase input currents; the three-phase AC side filter inductor L_a=L_b=L_c=L; and R denotes the equivalent resistance of the filter inductor and the switches. The output DC voltage is U_{dc}. The load resistance R_L and the DC-link capacitor C are connected to the DC side of the converter, where i_L=U_{dc}/R_L denotes the load current. The resonant inductor L_r is resonant with the switches parallel capacitors C_1-C_7 to create the condition of soft switching and to suppress the diode reverse recovery current. C_c denotes clamping capacitor, which forms the clamp branch together with switch S_7 and resonant inductor L_r to reduce the voltage stress across the switches.

The switching function of the bridge leg is defined as S_i(i=a, b, c), where S_a=1 means that S_1 is on, and S_2 is off. Meanwhile, S_a=0 means that S_1 is off, and S_2 is on.

Based on the working principle of a CACZVS three phase PFC converter [1], it is known that during most of the operation time, the auxiliary switch S_7 is conducting. S_7 is turned off in a very short time to create the zero voltage switching condition for the main switches. This does not affect the main circuit during the rest time. Therefore, the state space equation of the CACZVS three phase PFC converter in the three phase stationary coordinate system can be written as [1]:

$$\begin{cases} L\dfrac{di_a}{dt} = U_a - Ri_a - \dfrac{2S_a - S_b - S_c}{3}(U_{dc} + U_{Cc}) \\ L\dfrac{di_b}{dt} = U_b - Ri_b - \dfrac{2S_b - S_a - S_c}{3}(U_{dc} + U_{Cc}) \\ L\dfrac{di_c}{dt} = U_c - Ri_c - \dfrac{2S_c - S_a - S_b}{3}(U_{dc} + U_{Cc}) \\ C\dfrac{dU_{dc}}{dt} = S_a i_a + S_b i_b + S_c i_c - i_L \end{cases}, \quad (1)$$

where U_{Cc} denotes the voltage crossing clamping capacitor C_c. By transforming Eq. (1) into the two-phase rotating coordinate

system, the following is obtained:

$$\begin{cases} L\dfrac{di_d}{dt} = U_d - Ri_d + wLi_q - S_d(U_{dc} + U_{Cc}) \\ L\dfrac{di_q}{dt} = U_q - Ri_q - wLi_d - S_q(U_{dc} + U_{Cc}) \\ C\dfrac{dU_{dc}}{dt} = \dfrac{3}{2}(S_d i_d + S_q i_q) - i_L \end{cases}, \quad (2)$$

where $w=2\pi f$ denotes the angular frequency of the input sinusoidal voltage, U_d, U_q denote the active and reactive voltage components in the *dq* coordinate system, respectively, i_d, i_q denote the active and reactive current components in the *dq* coordinate system, respectively, and S_d, S_q denote the switching functions in the *dq* coordinate system, respectively. Because C_c<<C, it is true that U_{Cc}<<U_{dc}. By ignoring U_{Cc}, it is possible to obtain:

$$\begin{cases} L\dfrac{di_d}{dt} = U_d - Ri_d + wLi_q - S_d U_{dc} \\ L\dfrac{di_q}{dt} = U_q - Ri_q - wLi_d - S_q U_{dc} \\ C\dfrac{dU_{dc}}{dt} = \dfrac{3}{2}(S_d i_d + S_q i_q) - i_L \end{cases}. \quad (3)$$

Based on Eq. (3), the PI controllers are designed in the next section.

III. Triple Close-Loop PI Controllers Design

A. Current Loop Controller Design

From Eq. (3), the current loop equation is given as:

$$\begin{cases} L\dfrac{di_d}{dt} = U_d - Ri_d + wLi_q - U_{rd} \\ L\dfrac{di_q}{dt} = U_q - Ri_q - wLi_d - U_{rq} \end{cases}, \quad (4)$$

where U_{rd}=$S_d U_{dc}$ and U_{rq}=$S_q U_{dc}$ denote the *d*-axis (active) and *q*-axis (reactive) current manipulating variables, respectively. The *d*-axis and *q*-axis current dynamics are nonlinear and strongly coupling. Therefore, traditional current feedback control based on the linear system theory cannot deal with such case. Here, it is possible to use the feed-forward decoupling PI control strategy for the current loop [3]. The controller equation is:

$$\begin{cases} U_{rd} = (k_{idp}e_{id} + k_{idi}\int_0^t e_{id}dt) + wLi_q - Ri_d + U_d \\ U_{rq} = (k_{iqp}e_{iq} + k_{iqi}\int_0^t e_{iq}dt) - wLi_d - Ri_q + U_q \end{cases}, \quad (5)$$

where i_{dref} is the *d*-axis current reference, and i_{qref} is the *q*-axis current reference, respectively, and e_{id}=i_d-i_{dref}, e_{iq}= i_q-i_{qref} denote the corresponding current errors. k_{idp}, k_{idi}, k_{iqp}, k_{iqi} are PI parameters. By substituting (5) into (4), it is possible to obtain:

$$\begin{cases} L\dfrac{di_d}{dt} + k_{idp}e_{id} + k_{idi}\int_0^t e_{id}dt = 0 \\ L\dfrac{di_q}{dt} + k_{iqp}e_{id} + k_{iqi}\int_0^t e_{id}dt = 0 \end{cases}. \quad (6)$$

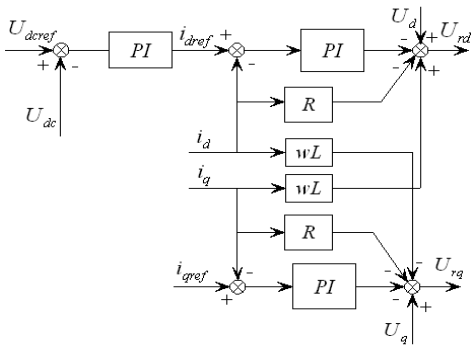

Fig. 2. Schematic of triple closed loop PI controller.

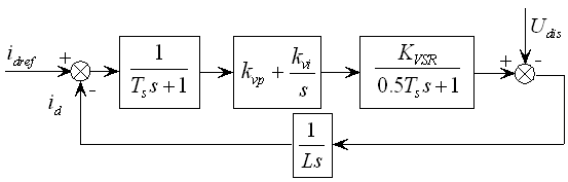

Fig. 3. Block diagram of the traditional PI current controller design [3].

The stability analysis shows that, as long as k_{idp}>0, k_{idi}>0, k_{iqp}>0, k_{iqi}>0, the feed-forward decoupling PI control strategy can make i_d track i_{dref}, and i_q track i_{qref}. In order to achieve a unity power factor, the reactive current i_q must be zero. Therefore, i_{qref}=0. i_{dref} is determined by the voltage loop controller. The function of the current loop controller is to make the input current sinusoidal and synchronous with the input voltage. At the same time, it should also make the active power of the converter have a quick response to load variations.

B. Voltage Loop Controller Design

From Eq. (3), the voltage loop equation is given as:

$$C\frac{dU_{dc}}{dt} = \frac{2}{3}(S_d i_d + S_q i_q) - i_L. \quad (7)$$

The voltage loop controller is:

$$i_{dref} = k_{vp}(U_{dcref} - U_{dc}) + k_{vi}\int_0^t (U_{dcref} - U_{dc})dt, \quad (8)$$

where U_{dcref} is the voltage reference, and k_{vp}, k_{vi} are the proportional and integral gains of the voltage PI controller, respectively.

To sum up, a block diagram of the triple closed loop PI controllers is shown in Fig. 2. Six control parameters, including k_{idp}, k_{idi}, k_{iqp}, k_{iqi}, k_{vp}, k_{vi} need to be tuned to obtain the desired performance. Moreover, the six parameters are mutually influenced. Therefore, they should be tuned coordinately to get better performance.

The traditional control parameter tuning method [3] simplified the synchronous reference-frame current control plant into a first-order time lag block. Then the linear control theory was used to design the control parameters. A block diagram of the traditional current control loop design is shown in Fig. 3, where U_{dis} denotes the voltage disturbance, and the PWM rectifier is treated as a first-order subsystem given by

$K_{VSR}/(0.5T_s s+1)$, where K_{VSR} denotes the equivalent gain of the rectifier, and T_s denotes the sampling period. The sampling process is modeled as a first-order subsystem given by $1/(T_s s+1)$. The AC block is modeled as a integral subsystem given by $1/Ls$, where the equivalent resistance R is omitted.

The traditional parameter tuning method, based on a lot of hypothesis and simplification, the voltage loop control parameters and the current loop control parameters are designed separately. Then the PI parameters need to be adjusted in a large range according to the designer experience. PI parameters obtained by the traditional method, generally speaking, make it impossible to achieve optimal performance.

IV. Triple Close Loop PI Controller Parameter Optimization Based on CPSO

A. Basic PSO

PSO is an optimization tool based on the principle of bird food searching, where each bird is treated as a particle, and each particle is a potential N-dimensional solution of the problem under consideration. There are M particles forming a population, the particles in the population coexist and cooperate. Each particle, with its velocity determined by the experience of itself and the "best experience" of the adjacent particles, flies to a "better" position in the solution space. In this way, the optimal solution is eventually found. The main parameters used in the PSO are shown in Table I.

The searching algorithm of particle m is given as follows:

$$V_{mn}(k+1) = wV_{mn}(k) + c_1 r_1 (Y_m(n) - X_{mn}(k)) + c_2 r_2 (Y_g(n) - X_{mn}(k)) \quad (9)$$

$$X_{mn}(k+1) = X_{mn}(k) + V_{mn}(k), \quad (10)$$

where $X_{mn}(k)$, $V_{mn}(k)$ denote the n^{th} coordinate position value and the n^{th} coordinate speed value of particle m at the k^{th} iteration, respectively. In the algorithm, V_{mn} is limited to within $\pm V_{max}$, which is set as 20% of the searching range of the particle. In this paper, a particle presents the 6-dimensional PIs parameters of the triple closed loop PI controllers.

B. Initial Population Generation Using the Unilateral Coupled Map Lattice

Based on the result in [21], the parameters w, c_1 and c_2 affect the convergence of the classical PSO algorithm. However, c_1 and c_2 are constant parameters, while the linearly or exponentially variant w can not ensure the ergodicity of the solution. In fact, the initial distribution of the particles has an important effect on the performance of the PSO. Non-uniform distribution of the initial particles might cause instability of the algorithm. In order to obtain a better initial distribution of the particles, chaotic logistics and a self-logical map have been proposed to generate the initial particles [16]-[19]. However, the most commonly used chaotic maps can only generate a one-dimensional uniform distribution of particles. For the application of a multi-dimensional optimization problem, such as the multiple control parameter optimization problem in this paper, the ideal situation is that the initial population (N-dimensional M-particles) is uniformly distributed in the entire solution space. However, the existing methods can hardly fulfill this requirement.

TABLE I
PSO Parameters Description

Parameter	Description
m	m=1,2,…,M is particle index
n	n=1,2,…,N is the dimension index of the solution space
k	iteration number
X_{mn}	n^{th} coordinate position value of particle m
V_{mn}	n^{th} coordinate speed value of particle m
Y_{mn}	the historical best n^{th} coordinate position value of particle m by itself
Y_{gn}	the historical global best n^{th} coordinate position value for all particles in the population
w	inertia weight
c_1, c_2	acceleration constants
r_1, r_2	independent random numbers

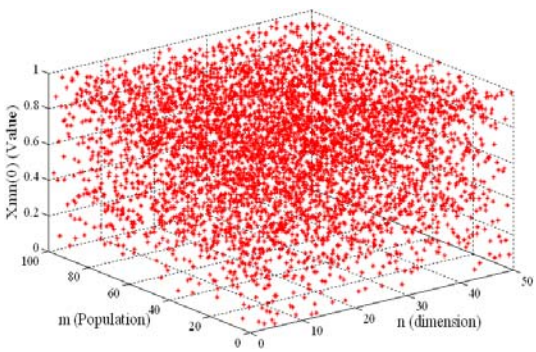

Fig. 4. Initial population generated by unilateral coupled map lattices.

In this paper, a unilateral coupled lattices spatiotemporal map is proposed to generate the initial particles. The unilateral coupled map lattices model is given as:

$$L_n(m+1) = (1-\varepsilon_n) f[L_n(m)] + \varepsilon_n f[L_{n-1}(m)], \quad (11)$$

where $f[L_n(k)]$ is the Logistic map, which is given by:

$$f[L_n(m)] = \mu L_n(m)(1-L_n(m)), \quad (12)$$

where $L_n(m)$ denotes the state variables, n denotes the space position (corresponding to the dimension of the particle), m denotes the discrete-time (corresponding to the population of the particle), μ is a constant, and ε_n denotes the coupling strength. Here, $X_{mn}=L_n(m)$. As a result, it is possible to use Eqs. (11) and (12) to generate the initial population of the proposed PSO.

The distribution chart of particles generated by the unilateral coupled map lattices is shown in Fig. 4.

Fig. 5 is a distribution comparison between the traditional logistic map and the proposed unilateral coupled map lattices spatiotemporal map. Figures 5 (a) and (b) are the box-plot

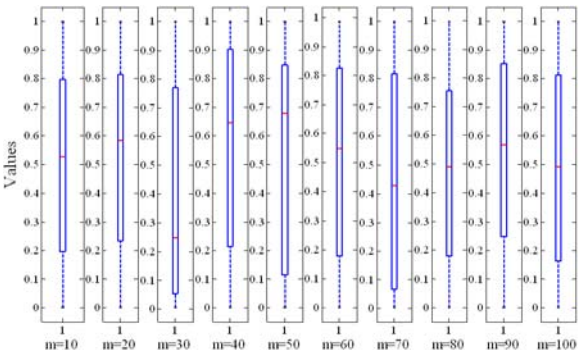

(a) boxplot of the proposed chaotic map.

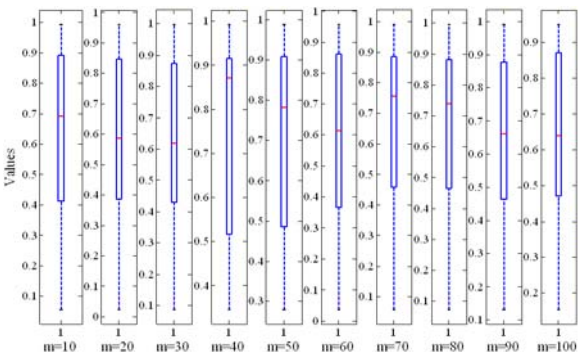

(b) boxplot of logistic map.

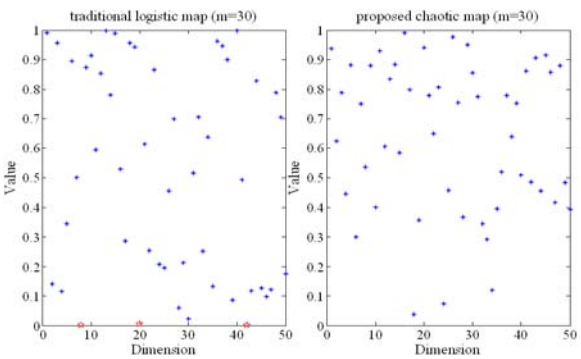

(c)

Fig. 5. Distribution comparison between the traditional logistic map and the proposed unilateral coupled lattices spatiotemporal map.

curves of the proposed method and the logistic map, respectively, where m is chosen as different values to see the degree of the uniform distribution, and the box length indicates the uniform distribution degree, i.e., the longer the box is, the better the uniform distribution is. From Figs. 5 (a) and (b), it can be seen that, for every value of m, the length of the corresponding box in Fig. 5(a) is larger than that in Fig. 5(b). This indicates the better performance of the proposed map when compared to the traditional logistic map. Figure 5(c) shows a comparison of the N-dimension elements between the proposed chaotic map and the traditional logistic map when m=30. From Fig. 5 (c), it can be seen that when compared to the traditional logistic map, the proposed method has tighter

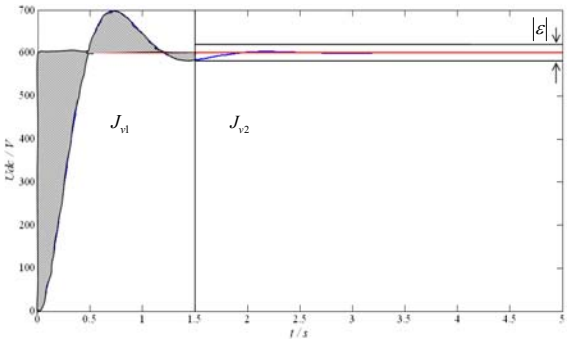

Fig. 6. Calculation of objective functions.

boundary conditions in the sense of no boundary point appearing in the "red star points" in the left subplot of Fig. 5 (c) (by using the logistic map).

In summary, by using the unilateral coupled lattices spatiotemporal chaotic map, the proposed CPSO algorithm in this paper can achieve a better distribution for the initial particles, which helps accelerate the convergence speed and avoid falling into a local optimum.

C. Objective Functions and Pareto Optimum Based Best Solution Selection

The objectives of the optimization problem in this paper are multi-fold, because the ideal performance of triple closed loop PI controllers needs to fulfill the following requirements: (1) a small raising time and a small overshoot; (2) zero steady state error; and (3) a unity power factor. The objectives of the voltage loop controller include two parts: firstly, the output DC voltage should approach the reference as soon as possible, and the corresponding overshoot should be as small as possible, i.e., the shadow area in Fig. 6 should be as small as possible. This objective is denoted as J_{v1} given by Eq. (13). Secondly, the steady-state error of the output voltage should be 0. This objective is denoted as J_{v2} given by Eq. (14). The objective of the current loop is to achieve a unity power factor. This is denoted as J_i given by Eq. (15).

$$J_{v1} = \frac{1}{\frac{1}{L_1}\sum_{i=1}^{L_1}|e_i|}, \tag{13}$$

$$J_{v2} = \frac{1}{\frac{1}{L_2}\sum_{i=L_1}^{L_1+L_2-1}|e_i|}, \tag{14}$$

$$J_i = \frac{1}{\frac{1}{L_3}\sum_{j=1}^{L_3}|e_j|}, \tag{15}$$

where e_i=$U_{dcref}(iT)$-$U_{dc}(iT)$ and e_j=$PF(jT)$-1 denote the voltage error and the power factor error, respectively, $PF(jT)$ denotes the power factor at the j^{th} sampling time, T is the sampling interval, and ε denotes the boundary of the steady-state error, which is used to distinguish the transient and steady state. L_1 represents the data length considered for the output DC voltage in the transient state. L_2 represents the data length considered

for the steady state of the output DC voltage, and L_3 is the data length considered for the power factor PF.

Clearly, for the optimization problem in this paper, there are three objectives. These objectives might have conflicts, and the increasing of one objective function might cause a decreasing of the other objectives (such as J_{v1} and J_{v2}). Balancing these objectives is a challenge task. The simplest way to solve a multi-objective optimization problem is giving different weights to different objectives and summing them together to form a single objective. In this way, it is possible to use the traditional single objective optimization algorithm to find the optimal solution. The drawback of this approach is the difficulty in choosing optimal weights for the multi-objectives. In fact, there exists a proper weight set to get the optimum solution only for convex optimization problems [20]. In order to solve these problems, an objective function based on the Pareto optimal solution theory is proposed.

To begin with, a definition about the domination (for the maximization problem) is given as follows:

***Domination*:** one solution X_1 dominates another solution X_2 for a optimizing problem, denoted as $X_1 > X_2$, if and only if

1) X_1 is not worse than X_2 for all of the objectives, i.e., $J_k(X_1) \geq J_k(X_2)$, where J_k is the k^{th} objective function.
2) X_1 is strictly better than X_2 for at least one objective, i.e., $\exists\, k = 1,2, \ldots, n_k,\ J_k(X_1) > J_k(X_2)$, where n_k is the number of objectives.

A non-dominated solution is a solution that is not dominated by any other solutions. A non-dominated solution is the best solution to a problem in the sense of no other solution being better than it. All non-dominated solutions form the Pareto non-dominated solutions set.

Unlike the classical PSO, non-dominated solutions are used as the individual best Y_m, and the global best Y_g. In other words, the global best and individual best are selected from the Pareto non-dominated solutions set for the proposed PSO.

D. Steps of the Proposed Algorithm

The detailed steps of the proposed multi-objective CPSO method are given as follows:

1) Initialize M particles with positions and velocities in the N-dimensional solution space using the proposed spatiotemporal chaos model. Then initialize the maximum number of iterations, k_{max}, and the initial global best.
2) For particle m in the k^{th} iteration, a six dimensional vector, consisting of $X_{m1}(k)$, $X_{m2}(k)$, $X_{m3}(k)$, $X_{m4}(k)$, $X_{m5}(k)$ and $X_{m6}(k)$ (representing the controller parameter vectors k_{vp}, k_{vi}, k_{idp}, k_{idi}, k_{iqp} and k_{iqi}), is used in the simulation model of a CACZVS three phase PFC converter to derive the output voltage response curve, the current response and the corresponding power factor. Then, the objective functions, including $J_{v1}(m, k)$, $J_{v2}(m, k)$ and $J_i(m, k)$, corresponding to particle m in the k^{th} iteration are calculated, where m=1, 2,…, M.
3) Compare the objective functions $J_{v1}(m,k)$, $J_{v2}(m,k)$, and $J_i(m,k)$ of particle m with its corresponding historical optimal objective functions (i.e. the best objective functions among all of the past iterations of particle m, given as $J_{v1\max}(m)$, $J_{v2\max}(m)$, and $J_{i\max}(m)$). If the following conditions are all satisfied, $J_{v1}(m,k) \geq J_{v1\max}(m)$, $J_{v2}(m,k) \geq J_{v2\max}(m)$ and $J_i(m,k) \geq J_{i\max}(m)$, then $J_{v1\max}(m) = J_{v1}(m,k)$, $J_{v2\max}(m) = J_{v2}(m,k)$, and $J_{i\max}(m) = J_i(m,k)$, at the same time. Because particle m is the new non-dominated solution, it is incorporated into a vector set referred to as an individual Pareto optimal set using $YY_m(ii)=\{X_{m1}, X_{m2}, X_{m3}, X_{m4}, X_{m5}, X_{m6}\}$, $ii=ii+1$, where YY_m denotes the individual Pareto optimal set of particle m (the best "experience" of itself), and ii denotes the row number of the particles in the individual Pareto optimal solution set. The individual best at the k^{th} iteration is randomly selected from YY_m, using $Y_m(1)=YY_m(randindex, 1)$, $Y_m(2)=YY_m(randindex, 2)$, $Y_m(3)=YY_m(randindex, 3)$, $Y_m(4)=YY_m(randindex, 4)$, $Y_m(5)=YY_m(randindex, 5)$, $Y_m(6)=YY_m(randindex, 6)$, *randindex* is randomly selected in the integer set [1, ii-1].
4) Compare the three objective functions of all the M particles in this iteration. If $J_{v1}(m, k) = \max_{i=1,\cdots M}\{J_{v1}(i, k)\}$, $J_{v2}(m, k) = \max_{i=1,\cdots M}\{J_{v2}(i, k)\}$ or $J_i(m, k) = \max_{i=1,\cdots M}\{J_i(i, k)\}$, then particle m is saved in a global Pareto optimal solution set using $P(jj)=\{X_{m1}, X_{m2}, X_{m3}, X_{m4}, X_{m5}, X_{m6}\}$, and the corresponding objective functions of particle m are also saved in a global objective function vector set using $O(jj,:)=[J_{v1}(m, k), J_{v2}(m, k), J_i(m, k)]$, then $jj=jj+1$, where P denotes the global Pareto optimal solution set, O denotes the global optimal objective function set, and jj denotes the row index of the set. Search in the global objective function set for the maximum value of each objective function, i.e., J_{v1gm}, J_{v2gm}, and J_{igm}. Then it is possible to obtain the global best $Y_g=P(j)=[X_{g1}, X_{g2}, X_{g3}, X_{g4}, X_{g5}, X_{g6}]$, where j is an index such that $\varepsilon(O(j, :), [J_{v1gm}, J_{v2gm}, J_{igm}]) = \min_{i=1,\ldots,jj-1}\varepsilon(O(i, :), [J_{v1gm}, J_{v2gm}, J_{igm}])$, where $\varepsilon(O(i, :), [J_{v1gm}, J_{v2gm}, J_{igm}])$ is a Euclidean distance, and $O(i, :)$ means the vector in the objective function value set corresponding to the i^{th} global Pareto optimal solution, which consists of $[O(i,1), O(i,2), O(i,3)]$. This operation means that a particle in the global Pareto optimal solution set is selected

as the global best, so that its three objective function values are the closest to the perfect objective functions values, i.e., $[J_{v1gm}, J_{v2gm}, J_{igm}]$.

5) Using the individual best derived in step 3) and the global best derived in step 4) to update the velocity and position of particle m according to Eqs. (9) and (10), then k=k+1.

6) Loop to step 2) until k=k_{max}, where k_{max} is the maximum iteration.

In [22], the global best is selected by calculating the average value of all of the particles in the global Pareto optimal solution set. Reference [23] divided the searching space into different hypercubes, where each hypercube had a chance of being selected (by the Roulette method). Within one hypercube the global best would be randomly selected from the intersection of this hypercube and the global Pareto optimal solution set. This method needs a greater computation cost. Reference [24] calculated the Euclidean distances, in every iteration, from particle m to each row in the global Pareto optimal solution set. The row in the Pareto optimal solution set which had the smallest distance is selected as the global guide for particle m. This method is very complicated in terms of computation. Compared with the existing methods used to select the global best in [22] [23] [24], the method proposed in this paper has a faster search speed and a larger possibility to obtain the true global best.

V. Simulation and Experimental Results

A. Simulation Results

A simulation model of a CACZVS three phase PFC converter with triple closed loop PI controllers is built by integrating PSIM and MATLAB as done in reference [25]. This simulation configuration has the following benefits: (1) Compared to MATLAB, PSIM uses an ideal device to build the model and it uses a simpler trapezoidal method to solve the system equation. Thus, the simulation speed is faster. In this paper, the optimization algorithm requires many iterations. Therefore, using this configuration can effectively save the simulation time. (2) When compared to the PSIM simulation environment, MATLAB provides greater flexibility in terms of the controller design, and it provides a facility for running the proposed CPSO algorithm.

The converter parameters used in the simulation are given as follows: the three-phase input voltage value U_{in}=220V; the three-phase input filter inductor L=20mH; the inductor equivalent resistance R=1Ω; the switch parallel capacitor C_1=C_2=...=C_7=2nF; the resonant inductor L_r=100μH; the clamp capacitor C_C=40μF; the output filter capacitor C=1500μF; the load resistor R_L=300Ω; the reference of the output voltage U_{dcref}=600V; and the switching frequency f=10kHz.

The parameters used in the proposed multi-objective CPSO are given as follows: the population size M=100, the maximum number of iterations k_{max}=10, the initial value of the particles are generated in [0, 1] by the unilateral coupled lattices spatiotemporal map, then they are transformed into the parameter range [0, PK_{max}] as the initial position, PK_{max} =5 in the following simulation, the learning factors c_1=2.5 and c_2=1.5, the inertia weight w=0.9, and the speed limit V_{max}=1. The coupling strength ε_n of the unilateral coupled map lattices is 0.85, and the initial values of the lattices are randomly chosen in [0, 1].

TABLE II
Performance Comparison of Different Methods

Initialization method	Average value			
	J_{v1}	J_{v2}	J_i	k_r
Random	0.12801	1.3442	21.0278	9.25
Logistic map	0.13577	1.3257	27.7862	8.654
Unilateral coupled map lattices	0.14393	1.3987	27.8081	8.5

TABLE III
Optimization Results of Different Methods

Value	Optimization method		
	Traditional PI tuning	Weighted CPSO	Proposed CPSO
k_{vp}	0.053025	0.037309	0.10664
k_{vi}	1.4546	1.5836	0.77894
k_{idp}	1.8671	1.2085	2.9229
k_{idi}	0.25412	1.1818	0.028256
k_{iqp}	2.0126	2.7516	4.1698
k_{iqi}	0.19868	1.2002	2.8368
J_{v1}	0.0389	0.0443	0.0466
J_{v2}	0.4045	0.5357	0.5784
J_i	31.651	41.6298	43.4745

In this paper, the proposed chaotic initialization method has the advantage of global convergence. In order to prove this, based on the same multi-objective PSO condition above but with different particles initialization methods, the comparison results using the random number in [14], the logistic map in [16], and the proposed chaotic map are shown in Table II. The results shown in Table II are the average values for running the optimization algorithm 50 times, where k_r denotes the average iteration times used for the different algorithms to reach stable optimized solutions. As can be seen from Table II, the traditional multi-objective PSO method in [14] (using the random initial particles) makes it easy to find a local optima because of the non-uniform distribution of the particles. Obviously, the proposed method has the highest average objective function and the fewest average iterations.

In order to verify the effectiveness of the proposed multi-objective optimization method, the PI parameters derived by the conventional method in [3] and fine tuning by the

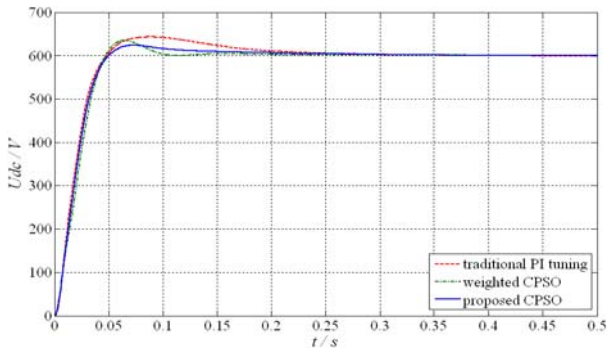

Fig. 7. Output DC voltage waveforms.

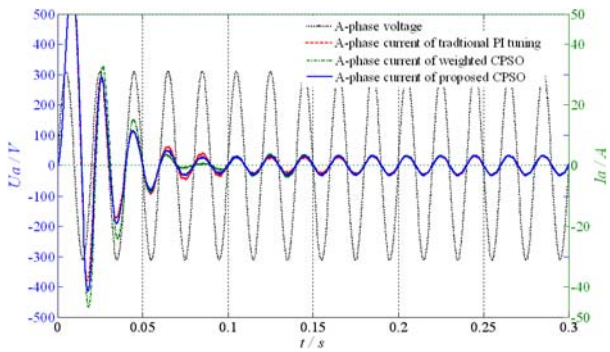

Fig. 8. The input A-phase voltage and the corresponding current waveforms.

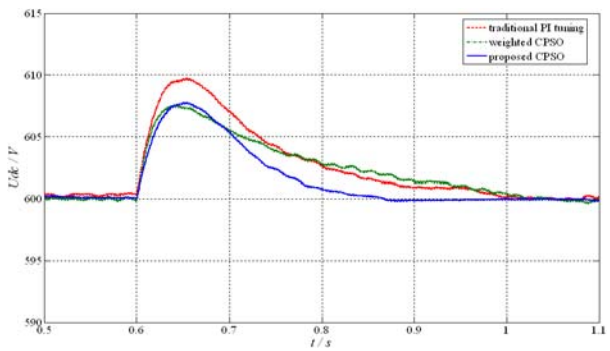

Fig. 9. Output dc voltage simulation waves when load changes.

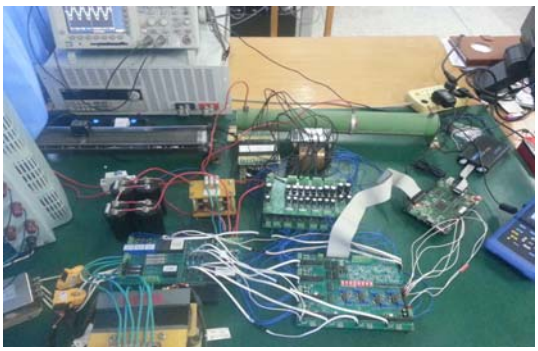

Fig. 10. Experimental platform photo.

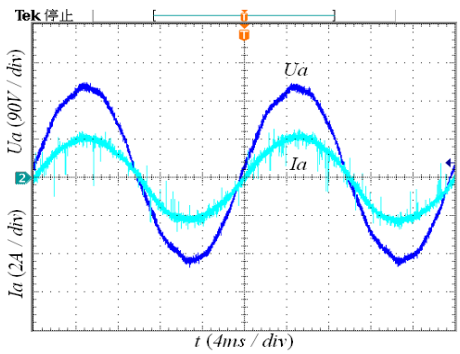

(a)

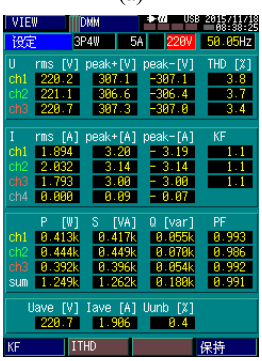

(b)

Fig. 11. Experiment result: (a) A-phase input voltage and current waveforms (b) result displayed by HIOKI 3197 power quality analyzer.

weighted multi-objective CPSO (the weighted function is $J=2J_{v1}+3J_{v2}+J_i$), and by the proposed multi-objective CPSO, are shown in Table III. It can be seen from Table III that the objective function values of the proposed method are the best.

The advantage of the Pareto optimal solution is automatically achieving balance among the different objectives in order to achieve better performance. The CACZVS three phase PFC converter output voltage waveforms are shown in Fig. 7 using the different PI parameters obtained by different methods in Table III. The input A-phase voltage and the corresponding current waveforms are shown in Fig. 8. From Figs. 7 and 8, the following conclusions can be obtained: the traditional PI parameter tuning method is very complicated and time consuming since it depends heavily on the designer's experience. The weighted multi-objective optimization method is simple and easy to operate. However, it is difficult to obtain the ideal weights to get the best results. The proposed method has the best performance. The output DC voltage has a smaller overshoot and no static state error. The input current of the proposed method settles down very quickly and achieves a unity power factor. Considering the performance of the voltage loop and current loop comprehensively, there is no doubt that the PI control parameters obtained by the proposed CPSO method are the best.

A load R_L variation from 300Ω to 450Ω is simulated, and the output DC voltage waveforms using the different PI parameters in Table III are shown in Fig. 9. From Fig. 9, it can be seen that the output perturbation is large and recovery time is long using the traditional PI tuning parameters. The performance of the weighted CPSO method is better than the

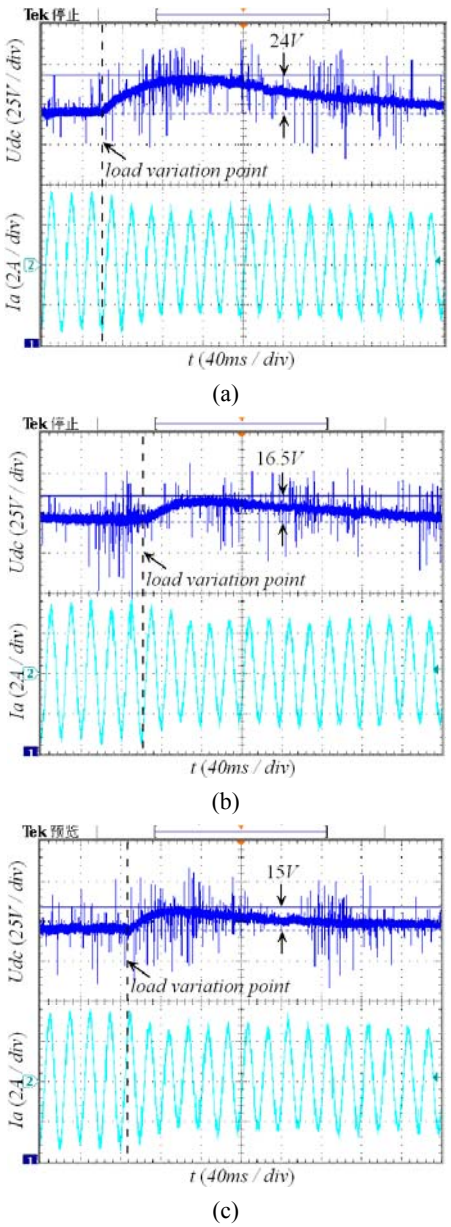

Fig. 12. Output DC voltage experimental waves when load changes. (a) Traditional PI tuning method. (b) Weighted CPSO method. (c) The proposed method.

traditional PI tuning method. The performance of the parameters obtained by the proposed method is the best.

B. Experiment Results

A 1.2kW hardware prototype is built as shown in Fig. 10. The control algorithms are programmed on a DSP28335 digital controller. The circuit parameters of the prototype are the same as those used in the simulation.

The CACZVS three phase PFC converter experiment results using the PI parameters obtained by the proposed multi-objective CPSO method are shown in Fig. 11. Fig. 11(a) shows the input A-phase voltage and the corresponding current waveforms, where the input current is synchronized with the input voltage. This indicates a unity power factor. Fig. 11(b) shows the display of a HIOKI3197 three-phase power quality analyzer, where the average three phase power factor is 0.991 and the three-phase total harmonic distortion THD <5%. This shows that the PI parameters obtained by the proposed optimization method work very well.

The experimental results corresponding to the simulation results in Fig. 9 are shown in Fig. 12. Fig. 12(a) shows the output DC voltage (channel 1) and the A-phase input current (channel 2) waveforms using the traditional tuning PI parameters. The output DC voltage perturbation is 24V and the voltage recovery time is about 0.36s. Fig. 12(b) shows the output DC voltage (channel 1) and the A-phase input current (channel 2) waveforms using the control parameters obtained by the weighted CPSO method. The output DC voltage perturbation is 16.5V and the voltage recovery time is about 0.3s. Figure. 12 (c) shows the output DC voltage (channel 1) and the A-phase input current (channel 2) waveforms using the control parameters obtained by the proposed method. The output DC voltage perturbation is 15V and the voltage recovery time is about 0.27s. Comparing three subplots in Fig. 12, it can be seen that the proposed method has the smallest output voltage perturbation and the shortest recovery time. The experiments results are consistent with the simulation results, which verifies the effectiveness and superiority of the proposed method.

VI. CONCLUSION

A CACZVS three phase PFC converter is used as an example for triple close loop PI controller parameter optimization. A multi-dimension multi-objective CPSO method is proposed to optimize the control parameters of the triple close loop PI controllers. For multi-dimensional particles, the unilateral coupled map lattices is proposed to produce the uniformly distributed initial particles in an N-dimension solution space. At the same time, for multi-objective functions, the Pareto optimal solution theory is applied to achieve balance among multiple objectives. The proposed chaos particle initialization method can realize a better initial distribution of particles in a multi-dimension solution space when compared to the traditional random number or one dimensional chaotic map. The proposed method avoids the difficulty of weight selection of the traditional weighted multi-objective optimization method. The propose method can be applied to optimize the control parameters. It can also be applied to the topology and parameter optimization of the circuits of the whole converter.

ACKNOWLEDGMENT

Supported in part by NSFC(61172070), SRFDP (20126118110008), Innovation Research Team of Shaanxi Province (2013KCT-04), Scientific Research Project of

Shaanxi Province (2013KW05-02), The Key Program of National Natural Science Foundation of China (61533014), Collaborative innovation program of Xi'an city(CXY1509-19), R &D Project of Beilin District of Xi'an City (GX1503).

REFERENCES

[1] H. P. Ren and X. Guo, "Robust adaptive control of CACZVS three phase PFC converter for power supply of silicon growth furnace," *IEEE Trans. Ind. Electron.*, Vol. 63, No. 2, pp. 903-912, Feb. 2016.

[2] M. J. L. Huber and M. Kumar, "Performance comparison of PI and P compensation in DSP based average current controlled three-phase six switch boost PFC rectifier," *IEEE Trans. Power Electron.,* Vol. 30, No. 12, pp. 7123-7137, Dec. 2015.

[3] V. Blasko and V. Kaura. "A new mathematical model and control of a three-phase AC-DC voltage source converter," *IEEE Trans. Power Electron.,* vol. 12, pp. 116-123, Jan. 1997.

[4] M. Perez, R. Ortega, and J. R. Espinoza, "Passivity-based PI control of switched power converters," *IEEE Trans. Control Syst. Technol.,* Vol. 12, No. 11, pp. 881-890, Nov. 2004.

[5] L. Corradini, P. Mattavelli, W. Stefanutti, and S. Saggini, "Simplified model reference-based auto tuning for digitally controlled SMPs," *IEEE Trans. Power Electron.,* Vol. 23, No. 7, pp. 1956-1963, Jul. 2008.

[6] X. W. Bao, F. Zhuo, Y. Tian, and P. Tan, "Simplified feedback linearization control of three-phase photovoltaic inverter with an LCL filter," *IEEE Trans. Power Electron.,* Vol. 28, No. 6, pp. 2739-2752, Jun. 2013.

[7] X. G. Zhang, W. J. Zhang, J. M. Chen, and D. G. Xu, "Deadbeat control strategy of circulating currents in parallel connection system of three-phase PWM converter," *IEEE Trans. Energy Convers.,* Vol. 29, No. 12, pp. 406-417, Jun. 2014.

[8] O. S. D. Oetinger and M. E. Magana, "Centralized model predictive controller design for wave energy converter arrays," *IET Renew. Power Gener.*, Vol. 9, No. 2, pp. 142-153, Feb. 2015.

[9] R. Guzman, L. Garcia de Vicuna, J. Morales, M. Castilla, and J. Matas, "Sliding-mode control for a three-phase unity power factor rectifier operating at fixed switching frequency," *IEEE Trans. Power Electron.,* Vol. 31, No. 1, pp. 758-769, Jan. 2016.

[10] Z. Song, W. Chen, and C. Xia, "Predictive direct power control for three-phase grid-connected converters without sector information and voltage vector selection," *IEEE Trans. Power Electron.,* Vol. 29, No. 10, pp. 5518-5531, Oct. 2014.

[11] Z. N. He, G. G. Yen, and J. Zhang, "Fuzzy-based Pareto optimality for many-objective evolutionary algorithms," *IEEE Trans. Evolut. Comput.*, Vol. 18, No. 4, pp. 269-285, April 2014.

[12] H. P. Ren and T. Zheng, "Optimization design of power factor correction converter based on genetic algorithm," in *Proc. ICGEC*, pp. 293-296, 2010.

[13] K.-B. Lee and J.-H. Kim, "Multi-objective particle swarm optimization with preference-based sort and its application to path following foot step optimization for humanoid robots," *IEEE Trans. Evolut. Comput.*, Vol. 17, No. 12, pp. 755-766, Dec. 2013.

[14] H. P. Ren and X. Guo, "Optimization controller design of CACZVS three phase PFC converter using particle swarm optimization," in *Proc. IECON*, pp. 1665-1671, 2014.

[15] Y. H. Shi and R. C. Eberhart, "Empirical study of particle swarm optimization," in *Proc. ECE*, pp. 1945-1950, 1999.

[16] B. Liu, L. Wang, Y. H. Jin, F. Tang, and D.-X. Huang, "Improved particle swarm optimization combined with chaos," *Chaos, Solitons and Fractals*, Vol. 25, No. 3, pp. 1261-1271, Mar. 2005.

[17] L. Y. Chuang, C. H. Yang, J. H. Tsai, and C.-H. Yang, "Operon prediction using chaos embedded particle swarm optimization," *IEEE/ACM Transactions on Computational Biology and Bioinformatics*, Vol. 10, No. 9, pp. 1299-1309, Sep. 2013.

[18] E. Mirzaei and H. Mojallali, "Auto tuning PID controller using chaotic PSO algorithm for a boost converter," in *Proc. IFSC,* pp. 1-6, 2013.

[19] C. P. Liu and C. M. Ye, "Mutative scale chaos particle swarm optimization algorithm based on self logical mapping function," *Application Research of Computers*, Vol. 28, No. 8, pp. 2825-2827, Aug. 2011.

[20] C. A. Coello, D. A. V. Veldhuizen, and G. B. Lamont, "Evolutionary algorithms for solving multi-objective problems," *Kluwer Academic Publishers*, 2002.

[21] M. Clerc and J. Kennedy, "The particle swarm: explosion stability and convergence in a multi-dimensional complex space," *IEEE Trans. Evolut. Comput.*, Vol. 6, No. 1, pp. 58-73, Feb. 2002.

[22] Y. Jin, M. Olhofer, and B. Sendhoff, "Dynamic weighted aggregation for evolutionary multi-objective optimization: Why does it work and how?," in *Proc. GECCO*, pp. 1042-1049, 2001.

[23] J. Zhang and H. Q. L, "A global-crowding-distance based multi-objective particle swarm optimization algorithm," in *Proc. CIS*, pp. 1-6, 2014.

[24] X. Hu, R. C. Eberhart, and Y. Shi, "Particle swarm with extended memory for multi-objective optimization," in *Proc. IEEE Swarm Intelligence Symposium*, pp. 193-197, 2003.

[25] J. Li, W. Wang, and Y. R. Zhong, "Joint simulation method of PSIM+MATLAB for power electronic systems," *Power Electronics*, Vol. 44, No. 5, pp. 86-88, May 2010.

Xin Guo was born in Xi'an, China, in 1986. He received his B.S. degree in Industrial Automation and his M.S. degree in Control Science and Engineering from the Xi'an University of Technology, Xi'an, China, in 2008 and 2011, respectively. He is presently working towards his Ph.D. degree in the School of Automation and Information Engineering, Xi'an University of Technology. He has published 5 journal papers and 3 IEEE conference papers. He is the holder of one Chinese patent. His current research interests include the design, analysis, and control of power electronic systems, and pneumatic servo systems.

Hai-Peng Ren was born in Heilongjiang, China, in March 1975. He received his Ph.D. degree in Power Electronics and Power Drives, from the Xi'an University of Technology, Xi'an, China, in 2003. He worked as a Visiting Researcher at Kyushu University, Fukuoka, Japan, from April

2004 to October 2004. He worked as Post-Doctoral Research Fellow in the field of time-delay systems at Xi'an Jiaotong University, Xi'an, China, from December 2005 to December 2008. He worked as an Honorary Visiting Professor at the University of Aberdeen, Aberdeen, Scotland, UK, from July 2010 to July 2011. He is presently working as a Professor at the Xi'an University of Technology. He obtained a National Invention Award (second prize) in 2012. He was the PI of more than 30 projects including 3 from the National Natural Science Foundation of China. He is the holder of 17 Chinese patents, and has 10 patents pending. He has published more than 80 papers, including papers for the PRL, IEEE TIE, IEEE TIA, IEEE TCBB, IEEE TCAS II, etc. His current research interests include nonlinear system control, complex networks and communication with nonlinear dynamics.

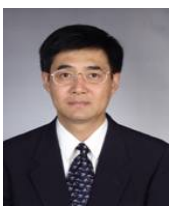

Ding Liu was born in China, in 1957. He received his B.S. and M.S. degrees from the Xi'an University of Technology, Xi'an, China, in 1982 and 1987, respectively, and his Ph.D. degree from Xi'an Jiaotong University, Xi'an, China, in 1997. From 1991 to 1993, he was a Visiting Scholar with the University of Fukui, Fukui, Japan. He has published more than 100 papers, including papers for the IEEE TSP, IEEE TAP, IEEE TCAS II, IEEE Sensors Journal, etc. His current research interests include complex system modeling and control, intelligent robot control, digital signal processing, and intelligent control theory.